

# Deep Virtual Compton Scattering and the Nucleon Generalized Parton Distributions.

M. Guidal<sup>a</sup>

<sup>a</sup>Institut de Physique Nucléaire, IN2P3, F-91406 Orsay, France,  
E-mail: guidal@ipno.in2p3.fr

In the following, the subject of Deep Virtual Compton Scattering on the nucleon and its relation to the recently introduced concept of Generalized Parton Distributions are briefly reviewed. The general theoretical framework and the links between theory and experiment will be outlined and the recently published data which look promising for the development of this field will be discussed. Finally, the experimental prospectives of the domain will be presented.

## 1. Introduction

The scattering of coherent light on an object (broadly speaking, Compton scattering) is one of the most elementary processes of physics. In a general way, by measuring the angular and energy distributions of the scattered light, information on the structure and the shape of the probed object can be accessed : for instance, the spatial or momentum distributions of its internal constituents, their spin distributions, etc... While such scattering can certainly be done with other incident particles, the advantageous feature of light (be it under the form of a wave or a photon particle) is its electromagnetic nature, which makes it interact with matter through the most precise theory we know, Quantum Electrodynamics (QED) at the most fundamental level.

The wavelength (inversely proportional to the energy) of the incident light must match the size of the probed object in order to be able to probe its internal structure. Over time, the scattering of light has been widely studied and used to probe objects of decreasing size (and therefore of increasing energy). In order to study the quark and gluon structure of the nucleon (i.e., the partons), incident beams on the GeV scale are needed to probe sizes of the order of a fermi. It is only recently, with the advent of intense multi-GeV lepton beam facilities, that it has become possible to experimentally study Compton scattering at the smallest dimensions of matter : the nucleon or quark and gluon level, where it is traditionally called Deep Virtual Compton Scattering (DVCS) -the term “virtual” here meaning that the incoming photon is radiated from a lepton beam, which presents the additional advantage of varying its 3-momentum independently of its energy-.

In parallel, only less than 10 years ago, the theoretical formalism has appeared, within the framework of QCD (“Quantum ChromoDynamics”, the theory governing the interaction between quarks and gluons), to interpret such reaction at the partonic level, through the concept of the “Generalized Parton Distributions” (GPDs). In the following, the

general theory and experimental status of DVCS, that is the Compton scattering at the nucleon level, shall be briefly presented.

## 2. Generalized Parton Distributions

### 2.1. Formalism

In the last decade, Mueller et al. [1], Ji [2] and Radyushkin [3] have shown that the leading order perturbative QCD (pQCD) amplitude for Deeply Virtual Compton Scattering in the forward direction can be factorized, in the Bjorken regime (i.e., in simplifying, large  $Q^2$ , where  $-Q^2$  is the squared mass of the virtual photon) in a hard scattering part, exactly calculable in pQCD or QED, and a nonperturbative nucleon structure part. This is illustrated in Fig. 1a). In these so-called “handbag” diagrams, the lower blob represents the unknown structure of the nucleon and can be parametrized, at leading order pQCD, in terms of 4 generalized structure functions, the GPDs. Using Ji’s notation, these are called  $H, \tilde{H}, E, \tilde{E}$ , and depend upon three variables :  $x, \xi$  and  $t$ . One considers the process in a frame where the proton has a large momentum along a certain direction which defines the longitudinal components.

$x + \xi$  is the longitudinal momentum fraction carried by the initial quark struck by the incoming virtual photon. Similarly,  $x - \xi$  relates to the final quark going back in the nucleon after radiating the outgoing photon. The difference in the longitudinal momentum fraction between the initial and final quarks is therefore  $-2\xi$ . In comparison to  $-2\xi$  which refers to purely *longitudinal* degrees of freedom,  $t$ , the squared 4-momentum transfer between the final nucleon and the initial one, contains *transverse* degrees of freedom (so-called “ $k_\perp$ ”) as well.

Intuitively, the GPDs represent the probability amplitude of finding a quark in the nucleon with a longitudinal momentum fraction  $x - \xi$  and of putting it back into the nucleon with a longitudinal momentum fraction  $x + \xi$  plus some transverse momentum “kick”, which is represented by  $t$ . Explicitly, the matrix element of the bilocal quark operator, representing the lower blob in Figs. 1a) and 1b), reads at leading twist :

$$\begin{aligned} & \frac{P^+}{2\pi} \int dy^- e^{ixP^+y^-} \langle p' | \bar{\psi}_\beta(-\frac{y}{2}) \psi_\alpha(\frac{y}{2}) | p \rangle \Big|_{y^+=\vec{y}_\perp=0} \\ &= \frac{1}{4} \left\{ (\gamma^-)_{\alpha\beta} \left[ H^q(x, \xi, t) \bar{N}(p') \gamma^+ N(p) + E^q(x, \xi, t) \bar{N}(p') i\sigma^{+\kappa} \frac{\Delta_\kappa}{2m_N} N(p) \right] \right. \\ & \quad \left. + (\gamma_5 \gamma^-)_{\alpha\beta} \left[ \tilde{H}^q(x, \xi, t) \bar{N}(p') \gamma^+ \gamma_5 N(p) + \tilde{E}^q(x, \xi, t) \bar{N}(p') \gamma_5 \frac{\Delta^+}{2m_N} N(p) \right] \right\}, \quad (1) \end{aligned}$$

where  $\psi$  is the quark field,  $N$  the nucleon spinor and  $m_N$  the nucleon mass. One uses a frame where the virtual photon momentum  $q^\mu$  and the average nucleon momentum  $P^\mu$  are collinear along the  $z$ -axis and in opposite directions.

The GPDs actually reveal a “double” nature : since negative momentum fractions are identified with antiquarks, one can define two regions according to whether  $|x| > \xi$  or  $|x| < \xi$ . In the region  $-\xi < x < \xi$ , one “leg” in Fig. 1a), represents a quark, and the other an antiquark. In this region, the GPDs behave like a meson distribution amplitude and can be interpreted as the probability amplitude of finding a quark-antiquark pair in the nucleon. This kind of information on  $q\bar{q}$  configurations in the nucleon and, more

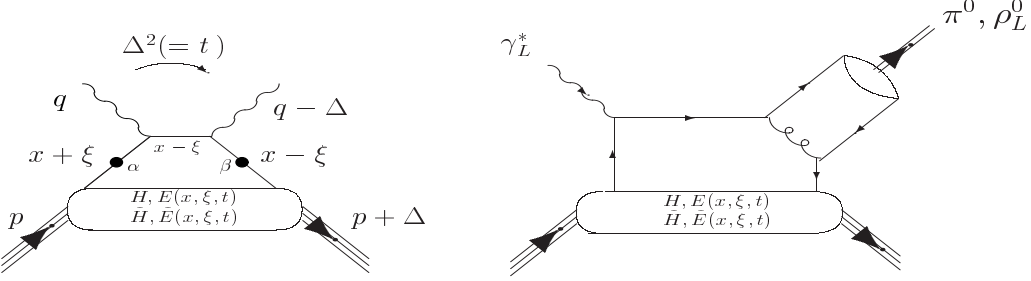


Figure 1. “Handbag” diagrams : a) for DVCS (left) and b) for meson production (right).

generally, the correlations between quarks (or antiquarks) of different momenta, all, being information carried in the concept of GPDs, are completely unknown at the time being, and reveal the richness and novelty of the GPDs.

In Eq.(1), one can see that  $H$  and  $E$  are independent of the quark helicity and are therefore called *unpolarized* GPDs, whereas  $\tilde{H}$  and  $\tilde{E}$  are helicity dependent and are called *polarized* GPDs. The GPD’s  $H^q, E^q, \tilde{H}^q, \tilde{E}^q$  are defined for a single quark flavor ( $q = u, d$  and  $s$ ). The GPDs  $H$  and  $\tilde{H}$  are actually a generalization of the parton distributions measured in deep inelastic scattering. Indeed, in the forward direction,  $H$  reduces to the quark distribution and  $\tilde{H}$  to the quark helicity distribution measured in deep inelastic scattering :

$$H^q(x, 0, 0) = q(x) , \quad \tilde{H}^q(x, 0, 0) = \Delta q(x) , \quad (2)$$

Furthermore, at finite momentum transfer, there are model independent sum rules which relate the first moments of these GPDs to the elastic form factors. By integrating Eq.(1) over  $x$ , one gets the following relations for one quark flavor :

$$\int_{-1}^{+1} dx H^q(x, \xi, t) = F_1^q(t) , \quad \int_{-1}^{+1} dx E^q(x, \xi, t) = F_2^q(t) , \quad (3)$$

$$\int_{-1}^{+1} dx \tilde{H}^q(x, \xi, t) = g_A^q(t) , \quad \int_{-1}^{+1} dx \tilde{E}^q(x, \xi, t) = h_A^q(t) . \quad (4)$$

where  $F_1$  and  $F_2$  are related to the nucleon electromagnetic form factors and  $g_A$  and  $h_A$  denote the axial and pseudoscalar form factors of the nucleon.

It has been shown [4–6] that the  $t$  dependence of the GPDs can be related, via a Fourier transform, to the transverse spatial distribution of the partons in the nucleon. At  $\xi=0$ , the GPD( $x, 0, t$ ) can be interpreted as the probability amplitude of finding in a nucleon a parton with *longitudinal* momentum fraction  $x$  at a given *transverse* impact parameter, related to  $t$ . In this way, the information contained in a traditionnal parton distribution, as measured in inclusive Deep Inelastic Scattering (DIS), and that contained within a form factor, as measured in elastic lepton-nucleon scattering, are now combined and correlated in the GPD description [7].

The second moment of the GPDs is relevant to the nucleon spin structure. It was shown in Ref.[2] that there exists a (color) gauge-invariant decomposition of the nucleon spin:

$$\frac{1}{2} = J_q + J_g , \quad (5)$$

where  $J_q$  and  $J_g$  are respectively the total quark and gluon spin contributions to the nucleon total angular momentum. The second moment of the GPD's gives

$$J_q = \frac{1}{2} \int_{-1}^{+1} dx x [H^q(x, \xi, t=0) + E^q(x, \xi, t=0)] , \quad (6)$$

and this relation is independent of  $\xi$ . The total quark spin contribution  $J_q$  decomposes as

$$J_q = \frac{1}{2} \Delta \Sigma + L_q , \quad (7)$$

where  $1/2 \Delta \Sigma$  and  $L_q$  are respectively the quark spin and quark orbital contributions to the nucleon spin. Since  $\Delta \Sigma$  has been measured through polarized DIS experiments (it is about 20%) and  $J_g$  is currently being measured at COMPASS and RHIC, a measurement of the sum rule of Eq.(6) in terms of the GPD's provides a model independent way of determining the quark orbital contribution to the nucleon spin, and therefore complete the “spin-puzzle”.

The GPDs reflect the structure of the nucleon independently of the reaction which probes the nucleon. They can also be accessed through the hard exclusive electroproduction of mesons - $\pi^0$ ,  $\rho^0$ ,  $\omega$ ,  $\phi$ , etc.- (see Fig. 1b)) for which a QCD factorization proof was given in Ref. [8]. In this case, the perturbative part of the diagram involves a 1-gluon exchange and therefore the strong running coupling constant, whose behavior at low energy scales is not fully controlled, makes the calculations and the interpretation of the data more complicated.

The current theoretical activity in the field bears mainly on the modelization of the GPDs within different frameworks (to name a few, the chiral quark soliton model [9], the constituent quark model [10,11], light-cone wavefunction overlap [12],...), on the control of the QCD corrections (Next to Leading Order evolution [13], higher twists [14,15], ....), on lattice calculations [16,17] and the extension of the formalism to processes other than the “hard” electroproduction of photons and mesons on the nucleon.

A non-exhaustive list of currently explored reactions is :  $\gamma p \rightarrow \gamma^* p$  [18] where  $\gamma^*$  decays into a lepton pair (*Timelike* Compton Scattering),  $\gamma^* p \rightarrow \gamma^* p$  [19,20] (*Double Deep Virtual* Compton Scattering),  $\gamma^* p \rightarrow \gamma \Delta$  [21] (*Resonant Deep Virtual* Compton Scattering),  $\gamma^* A \rightarrow \gamma A$  [24,25,22,23] (*Nuclear Deep Virtual* Compton Scattering),  $\gamma p \rightarrow \gamma p$  [26,27] (*Real* Compton Scattering),  $\bar{p}p \rightarrow \gamma \gamma$  [28] (*Inverse* Compton Scattering) -however, for these 2 last processes, RCS and ICS, the factorisation proof still remains to be established-, “hard” hybrid electroproduction [29], “hard” pentaquark electroproduction [30], etc...

We refer to Refs. [31,32] for very complete recent reviews of the field and more details on all these aspects which cannot be covered in this short contribution.

## 2.2. From theory to experiment

As mentioned in the previous section, the GPDs depend on three variables :  $x$ ,  $\xi$  and  $t$ . However, it has to be realized that only two of these three variables are accessible

experimentally, i.e.  $\xi$  (fully defined by detecting the scattered lepton  $\xi = \frac{x_B}{2-x_B}$ , where  $x_B$  is the traditional Bjorken variable used in DIS) and  $t$  (fully defined by detecting either the recoil proton or the outgoing photon or meson). However,  $x$  (which is different from  $x_B$  !) is a variable which is integrated over, due to the loop in the handbag diagrams (see Fig. 1). This means that, in general, a differential cross section will be proportional to :  $| \int_{-1}^{+1} dx \frac{H(x,\xi,t)}{x-\xi+i\epsilon} + \dots |^2$  (where ... stands for similar terms for  $E$ ,  $\tilde{H}$ ,  $\tilde{E}$  ;  $\frac{1}{x-\xi+i\epsilon}$  is the propagator of the quark between the incoming virtual photon and the outgoing photon -or meson-, see Fig. 1). In general, one will therefore measure integrals (with a propagator as a weighting function) of GPDs.

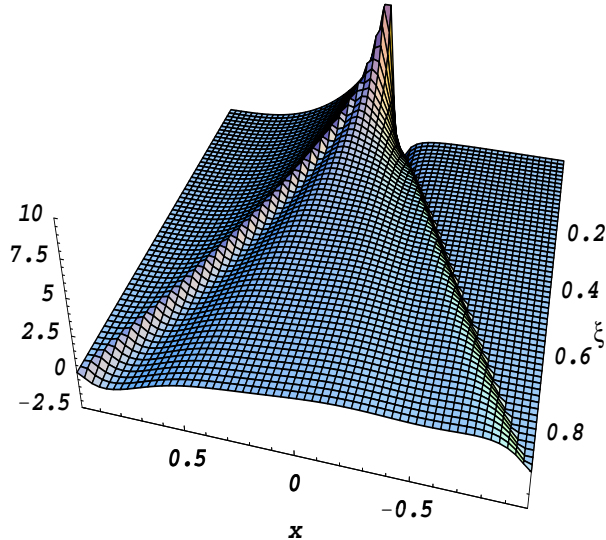


Figure 2. One model [31,33] for the GPD  $H$  as a function of  $x$  and  $\xi$  for  $t=0$ . One recognizes for  $\xi=0$  the typical shape of a parton distribution (with the sea quarks rising as  $x$  goes to 0, the negative  $x$  part being interpreted as the antiquark contribution). The figure is taken from Ref. [31].

To illustrate this point, Fig. 2 shows one particular model [31,33] for the GPD  $H$  as a function of  $x$  and  $\xi$  (at  $t = 0$ ). One identifies at  $\xi = 0$  a standard quark density distribution, with the rise around  $x = 0$  corresponding to the diverging sea contribution. The negative  $x$  part is related to antiquarks. One sees that the evolution with  $\xi$  is not trivial and that measuring the integral over  $x$  of a GPD, at constant  $\xi$ , will not define it uniquely .

A particular exception is when one measures an observable sensitive to the *imaginary* part of the amplitude, for instance, the beam spin asymmetry -BSA- in DVCS. It is non-zero at leading order due to the interference with the Bethe-Heitler process (see section 3.1). Then, since the amplitude  $\int_{-1}^{+1} dx \frac{H(x,\xi,t)}{x-\xi+i\epsilon} = PP(\int_{-1}^{+1} dx \frac{H(x,\xi,t)}{x-\xi}) - i\pi H(\xi,\xi,t)$ , one actually measures the GPDs directly at some specific point,  $x = \xi$  (i.e.,  $H(\xi,\xi,t)$ ). Consequently, measuring an observable that is sensitive to the real part of the amplitude (for instance, the beam charge asymmetry for DVCS) gives access to  $\int_{-1}^{+1} dx \frac{H(x,\xi,t)}{x-\xi}$ .

For mesons, transverse target polarization observables are also sensitive to a different combination of GPDs, namely combinations of the type :  $\int_{-1}^{+1} dx \frac{H(x,\xi,t)}{x-\xi} \times E(\xi,\xi,t)$ . The exact formula is more complicated, see for instance Ref. [21,31]. Such transverse spin asymmetries are sensitive to a *product* of the GPDs, as opposed to a sum of their squares, as is the case for a typical differential cross section.

It will therefore be a non-trivial task to actually extract the GPDs from the experimental observables as one actually only accesses, in general, weighted integrals of GPDs, or GPDs at some very specific points, or the product of these two. In the absence of any model-independent “deconvolution” procedure at this time, one has to rely on some global model fitting procedure.

As previously mentioned, GPDs are defined for one quark flavor  $q$  (i.e.  $H^q, E^q, \dots$ ) in a way similar to standard quark distributions. This flavor separation can be done through the measurement of several isospin channels ; for example,  $\rho^0$  production is proportional to  $2/3H^u + 1/3H^d$  (in a succinct notation) while  $\omega$  production is proportional to  $2/3H^u - 1/3H^d$ . Similar arguments apply to the polarized GPDs with the  $\pi^{0,\pm}, \eta, \dots$  channels. Similarly, DVCS on the proton and on the neutron probe different flavor combinations of the GPDs.

In summary, a full experimental program aiming at the extraction of the individual GPDs is a broad project which requires the study of several isospin channels and several observables, each having its own characteristics. Only a global study and fit to all this information may allow an actual extraction of the GPDs.

### 3. Experimental aspects

Over the last 20 years, most of what we have learned on the structure of the nucleon has come from the inclusive scattering of high energy leptons on the nucleon. By detecting only the scattered electron, a tremendous amount of information has already been obtained : apart from having shown the quark and gluon substructure of the nucleon, these experiments have shown that, for instance, about half of its momentum is carried by the quarks (the other half being carried by gluons) and that, as has been mentioned earlier, no more than about 20% of the spin of the nucleon originates from the quarks’ intrinsic spin.

Processes such as DVCS (or more generally meson leptonproduction reactions) require the determination of a particular final state : not only must the scattered electron be detected but also the whole final state. This is termed as an exclusive reaction.

The advent of the new generation of high-energy, high-luminosity lepton accelerators combined with large acceptance and high resolution spectrometers has recently given rise to the possibility of unambiguously measuring these exclusive low cross-section processes. We now discuss the first experimental results which have emerged in recent years and the new prospectives opening up.

#### 3.1. Recent experimental results

It is only in the past 3 years that some experimental results relevant to GPD physics, and of sufficient precision, have been obtained.

Fig. 3 shows the first measurement of the BSA for DVCS on the proton by HERMES

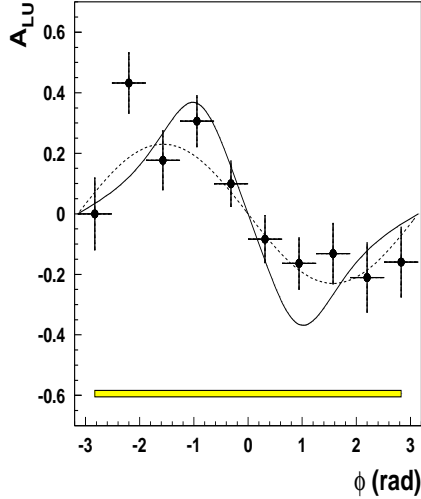


Figure 3. The DVCS beam asymmetry as a function of the azimuthal angle  $\Phi$  as measured by HERMES [34]. Average kinematics are :  $\langle x_B \rangle = .11$ ,  $\langle Q^2 \rangle = 2.6 \text{ GeV}^2$  and  $\langle -t \rangle = .27 \text{ GeV}^2$ . The dashed curve is a  $\sin\Phi$  fit whereas the solid curve is the theoretical GPD calculation of Ref. [15].

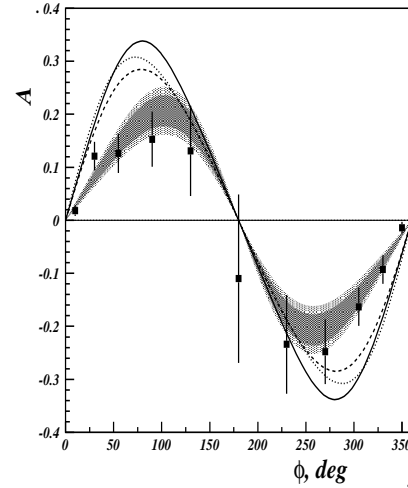


Figure 4. The DVCS beam asymmetry as a function of the azimuthal angle  $\Phi$  as measured by CLAS [39]. Average kinematics are :  $\langle x_B \rangle = .19$ ,  $\langle Q^2 \rangle = 1.25 \text{ GeV}^2$  and  $\langle -t \rangle = .19 \text{ GeV}^2$ . The shaded regions are error ranges for  $\sin\Phi$  and  $\sin 2\Phi$  fits. Calculations are : leading twist *without*  $\xi$  dependence [40,33] (dashed curve), leading twist *with*  $\xi$  dependence [40,33] (dotted curve) and leading twist + twist-3 [15] (solid curve).

with a 27 GeV positron beam. This asymmetry arises from the interference of the “pure” DVCS process (where the outgoing photon is emitted by the nucleon) and the Bethe-Heitler (BH) process (where the outgoing photon is radiated by the incoming or scattered lepton). The two processes are experimentally indistinguishable and interfere. The cross section will therefore be proportionnal to the squared amplitude :  $| M_{DVCS} + M_{BH} |^2$  while the difference between cross sections for different beam helicities will be proportional to :  $| M_{DVCS} \times M_{BH} |$ . The BH process being exactly calculable in QED, this latter observable therefore gives access in a *linear* fashion to the GPDs. The difference of cross sections for different beam helicities is also sensitive to the imaginary part of the amplitude : the BH being purely real, the GPD is measured in this way at the kinematical point ( $x = \xi, \xi, t$ ) as mentioned in a previous section.

The beam asymmetry, which is this latter difference of cross sections divided by their sum, is more straightforward to access experimentally since normalization and systematic issues cancel, in a first order approximation, in the ratio. For this asymmetry, a shape close to  $\sin\Phi$  (not an exact  $\sin\Phi$  shape as higher twists and the Bethe Heitler have some more complex  $\Phi$  dependence) is expected, where  $\Phi$  is the angle between the leptonic and the hadronic plane. At HERMES, the average kinematics is  $\langle x_B \rangle = .11$  ( $x_B$  is related to  $\xi$ , see section 2.2),  $\langle Q^2 \rangle = 2.6 \text{ GeV}^2$  and  $\langle -t \rangle = .27 \text{ GeV}^2$  for which an amplitude

of .23 for the  $\sin\Phi$  moment is extracted from the fit [34]. The discrepancy between the theoretical prediction and the data in Fig. 3 can certainly be attributed, in part, to the large kinematical range over which the experimental data have been integrated, and where the model can vary significantly, but also to higher twist corrections not yet calculated (so far, only twist-3 corrections are under theoretical control for this process, the leading twist being twist-2). See for instance Refs. [15,35,36] for more discussion on twist-3 accuracy in the DVCS process and Refs [37,38] about beam spin asymmetry in general.

The DVCS reaction at HERMES is identified by detecting the scattered lepton (positron) and the outgoing photon from which the missing mass of the non-detected proton is calculated. Due to the limited resolution of the HERMES detector, the selected peak around the proton mass is  $-1.5 < M_X < 1.7$  GeV, which means that contributions to this asymmetry from nucleon resonant states as well, cannot be excluded.

This same observable, i.e. the DVCS BSA on the proton, has been measured at JLab with a 4.2 GeV electron beam and the  $4\pi$  CLAS detector [39]. Due to the lower beam energy compared to HERMES, the kinematical range accessed at JLab is different :  $< x_B >=.19$ ,  $< Q^2 >=1.25$  GeV $^2$  and  $< -t >=.19$  GeV $^2$ . In this case, the DVCS reaction was identified by detecting the scattered lepton and the recoil proton. The missing mass of the photon was then calculated. Due to the geometry of the CLAS detector, outgoing photons emitted at very forward angles escape detection. The contamination by  $ep \rightarrow ep\pi^0$  events can be estimated to some extent, and subtracted bin per bin, resulting in a relatively clean signature of the exclusivity of the reaction.

Figure 4 shows the CLAS measured asymmetry along with theoretical calculations (predictions). They are in fair agreement. The different sign of the CLAS BSA relative to HERMES is due to the use of electron beams in the former case compared to positron beams in the latter. Again, discrepancies can be assigned to the fact that the theory is calculated at a single, well-defined, kinematical point whereas data have been integrated over several variables and wide ranges. Furthermore, Next to Leading Order as well twist-4 corrections which may be important at these rather low  $Q^2$  values, still need to be quantified.

This DVCS BSA on the proton has also been measured at higher energies, using beams of 4.8 GeV and 5.75 GeV, by the CLAS collaboration and preliminary results are currently being presented at conferences (see for instance Ref. [41]).

DVCS cross sections on the proton have, so far, only been measured at very high energies, by the H1 and ZEUS collaborations [42], where gluon contributions dominate. They still lend themselves to GPD interpretation through gluon exchange type processes [43] and, again, good agreement is found.

Besides BSA and cross sections, preliminary results for other observables are regularly presented in conferences : the DVCS beam charge asymmetry (which is sensitive to the real part of the amplitude, see section 2.2) has been measured on the proton at HERMES [44] and the proton target asymmetry at CLAS [41]. Also, first results of DVCS on nuclear targets are being released [44].

All these experimental results are very encouraging in the sense that the observed signals, although integrated over quite wide kinematical ranges, are generally compatible (in magnitude and in shape) with theoretical calculations. It should be underlined that almost all the calculations presented were actual *predictions* and were published before

the experimental results. The statistics of all the current measurements are, however, not high enough to allow for a fine binning of the kinematical variables and therefore do not allow as yet a precise test of the different GPD models.

### 3.2. The Prospectives

In the short-term, new results are soon to be expected from JLab, using the highest beam energy available. In Hall A, equipped with high resolution arm-spectrometers, two dedicated DVCS experiments [45,46] will measure with high precision some particular kinematical configurations ; the experiment actually started in fall 2004. In Hall B, equipped with a large acceptance spectrometer, a DVCS experiment [47] will allow to cover a broad phase space ; the experiment is scheduled to start data taking in spring 2005. These experiments are specialized in the sense that they will use special additional detectors, designed to detect the full final state of the reaction  $ep \rightarrow e'p\gamma$ . This will suppress the background coming from the contamination of additional pions. In particular, the Hall B experiment will use a forward angle electromagnetic calorimeter of about 400  $PbWO_4$  crystals ( $\approx 1 \times \approx 1 \times \approx 16 \text{ cm}^3$ ) equipped with Avalanche Photodiodes (APDs) designed to operate in strong magnetic fields. They will be used to detect the DVCS photons and unambiguously sign the exclusivity of the reaction. A successful one-week run took place in winter 2003 at JLab with a prototype, thus validating this new technique. The forthcoming program at JLab also plans to simultaneously measure the DVCS BSA on a deuterium/neutron target.

At HERMES, there is a project [48,44,41] to install in 2005 a recoil detector for the detection of the recoiling hadronic state. This should ensure the exclusivity of the reaction.

COMPASS, with a 100 to 200 GeV beam, has the unique feature of potentially accessing small  $x_B$  at sufficiently large  $Q^2$  and could also contribute to the field of GPDs. An experimental project is currently under study [49]. A dedicated recoil detector would also be installed in order to detect all the final particles of the DVCS process. Such a program could be envisaged to start around 2009.

While an exploratory study of the GPDs is under way at JLab ( $E_e=6 \text{ GeV}$ ) and HERMES ( $E_e=27 \text{ GeV}$ ), and could be envisaged in the future at COMPASS ( $E_\mu=100-200 \text{ GeV}$ ), it will probably not be sufficient to fully reveal the full GPD physics. A lepton accelerator facility combining a high luminosity ( $\approx 10^{35-36} \text{ cm}^{-2} \text{ s}^{-1}$  desirable) and a high energy beam ( $\approx 30 \text{ GeV}$ ) with a good resolution detector (a few tens of MeV for a typical missing mass resolution) would be appropriate.

The JLab upgrade [50] with an 11 to 12 GeV beam energy project, planned for 2008, promises to be the facility suited to a physics program devoted to the systematic study of exclusive reactions and the GPDs. It meets many of the requirements needed for this “exclusive” physics which are :

- Large kinematical range : it is desirable to span a domain in  $Q^2$  and  $x_B$  as large as possible. Although a higher beam energy would be even better, 11 GeV allows to reach  $x_B$  down to 0.1 and  $Q^2$  up to 8 GeV $^2$ .
- High luminosity : cross sections fall sharply with  $Q^2$  ; for a large acceptance detector, luminosities up to  $10^{35} \text{ cm}^{-2} \text{ s}^{-1}$  are necessary,
- Good resolution : it is important to cleanly identify exclusive reactions. This can

be achieved with a good resolution using the missing mass technique and/or by detecting all the final state particles and thus overdetermining the kinematics of the reaction. The CLAS++ upgrade project of the JLab large acceptance detector of Hall B is perfectly suited to achieving these goals.

Figure 5 summarizes the phase space covered by the current and short-term future projects related to this physics and clearly illustrates the complementarity of each.

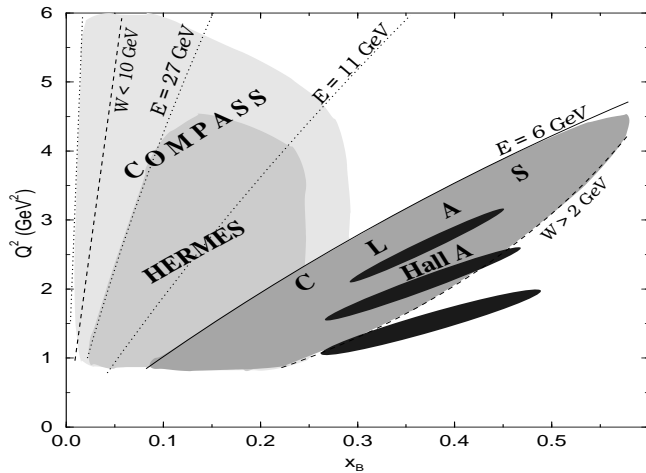


Figure 5.  $(Q^2, x_B)$  phase space covered by the current and short-term future experimental projects for DVCS. The figure is taken from Ref. [47].

#### 4. Conclusion

In conclusion, we believe that Compton scattering, from the nucleon down to the quark and gluon level and its theoretical interpretation in terms of GPD, open a broad new area in the investigation of the nucleon structure. GPDs allow to access new information in this field such as momentum and space correlations between quarks, quarks' orbital momentum and quark-antiquark configurations in the nucleon.

The first experimental results on DVCS, from the JLab, HERMES and H1/ZEUS facilities are encouraging and indicate that the manifestations of the handbag diagrams, that is to say Compton scattering at the quark level, are being seen. Now, dedicated programs at the existing facilities with special equipment and detectors have started and will soon yield a wealth of new experimental data. A full study aiming at the extraction of these GPDs from experimental data probably requires a new devoted facility providing high energy and high luminosity lepton beams, equipped with large acceptance and high resolution detectors. JLab with an 11 to 12 GeV beam energy is probably where the future of this field lies.

The author wishes to thank M. Vanderhaeghen, B. Pire and M. Mac Cormick for useful discussions.

## REFERENCES

1. D. Muller, D. Robaschik, B. Geyer, F. M. Dittes and J. Horejsi, Fortsch. Phys. **42** (1994) 101.
2. X. Ji, Phys. Rev. Lett. **78** (1997) 610; Phys. Rev. D **55** (1997) 7114.
3. A.V. Radyushkin, Phys. Lett. B **380** (1996) 417; Phys. Rev. D **56** (1997) 5524.
4. M. Burkardt, Phys. Rev. D **62**, 071503 (2000) [Erratum-ibid. D **66**, 119903 (2002)] ; Int. J. Mod. Phys. A **18**, 173 (2003).
5. M. Diehl, Eur. Phys. J. C **25**, 223 (2002) [Erratum-ibid. C **31**, 277 (2003)].
6. J. P. Ralston and B. Pire, Phys. Rev. D **66**, 111501 (2002).
7. A. V. Belitsky, X. d. Ji and F. Yuan, Phys. Rev. D **69**, 074014 (2004).
8. J.C. Collins, L. Frankfurt and M. Strikman, Phys. Rev. D **56** (1997) 2982.
9. V. Y. Petrov et al., Phys. Rev. D **57** (1998) 4325.
10. S. Scopetta and V. Vento, Eur. Phys. J. A **16**, 527 (2003)
11. S. Boffi, B. Pasquini and M. Traini, Nucl. Phys. B **649**, 243 (2003).
12. M. Diehl, T. Feldman, R. Jakob and P. Kroll, Nucl. Phys. B **596**, 33 (2001) [Erratum-ibid. B **605**, 647 (2001)].
13. L. Frankfurt, A. Freund, V. Guzey and M. Strikman, Phys. Lett. B **418**, 345 (1998) [Erratum-ibid. B **429**, 414 (1998)].
14. A. Freund, Phys. Rev. D **68**, 096006 (2003).
15. N. Kivel, M. V. Polyakov and M. Vanderhaeghen, Phys. Rev. D **63** (2001) 114014.
16. LHPC, P. Hagler, J. W. Negele, D. B. Renner, W. Schroers, T. Lippert and K. Schilling, Phys. Rev. Lett. **93** (2004) 112001.
17. M. Gockeler et al., hep-lat/0410023.
18. E. Berger, M. Diehl and B. Pire, Eur. Phys. J. C **23**, 265 (2001) [Erratum-ibid. C **31**, 277 (2003)].
19. M. Guidal and M. Vanderhaeghen, Phys. Rev. Lett. **90** (2003) 012001;
20. A. Belitsky and D. Muller, Phys. Rev. Lett. **90** (2003) 022001; Phys. Rev. D **68**, 116005 (2003).
21. L. Frankfurt, M. Polyakov, M. Strikman and M. Vanderhaeghen, Phys. Rev. Lett. **84** (2000) 2589;
22. S. Scopetta, Phys. Rev. C **70**, 015205 (2004).
23. F. Cano and B. Pire, Eur. Phys. J. A **19**, 423 (2004)
24. A. Kirchner and D. Muller, Eur. Phys. J. C **32**, 347 (2003)
25. M. Polyakov, Phys. Lett. B **555**, 57 (2003).
26. A.V. Radyushkin, Phys. Rev. D **58**, 114008 (1998).
27. M. Diehl, T. Feldman, R. Jakob and P. Kroll, Eur. Phys. J. C **8**, 409 (1999)
28. A. Freund, A.V. Radyushkin, A. Schafer and C. Weiss, Phys. Rev. Lett. **90** (2003) 092001;
29. I. Anikin et al., Phys. Rev. D **70**, 011501 (2004).
30. M. Diehl, B. Pire and L. Szymanowski, Phys. Lett. B **584** (2004) 58.
31. K. Goeke, M. V. Polyakov and M. Vanderhaeghen, Prog. Part. Nucl. Phys. **47** (2001) 401.
32. M. Diehl, Phys. Rept. **388** (2003) 41.
33. M. Vanderhaeghen, P.A.M. Guichon, M. Guidal, Phys. Rev. Lett. **80** (1998) 5064,

Phys.Rev. D **60** (1999) 094017.

34. A. Airapetian et al., Phys. Rev. Lett. **87** (2001) 182001.
35. I. Anikin et al, Phys. Rev. D **62**, 071501 (2000).
36. A. V. Belitsky and D. Muller, Nucl. Phys. B **589**, 611 (2000).
37. M. Diehl et al, Phys. Lett. B **411**, 193 (1997).
38. A. V. Belitsky, D. Muller, L. Niedermeier and A. Schafer, Nucl. Phys. B **593**, 289 (2001).
39. S. Stepanyan et al., Phys. Rev. Lett. **87** (2001) 182002.
40. P.A.M. Guichon and M. Vanderhaeghen, Prog. Part. Nucl. Phys. **41** (1998) 125.
41. F. Sabatie, talk at Baryons04 conference (Oct. 2004), “<http://baryons04.in2p3.fr>” and associated proceedings -to be published in Nucl. Phys. A-.
42. L. Favart, DIS 2001 Proceedings, hep-ex/0106067.
43. L. Frankfurt, A. Freund and M. Strikman, Phys. Rev. D **58** (1998) 114001 and Phys. Rev. D **59** (1999) 119901E.
44. M. Dueren, talk at Baryons04 conference (Oct. 2004), “<http://baryons04.in2p3.fr>” and associated proceedings -to be published in Nucl. Phys. A-.
45. P.-Y. Bertin, C. E. Hyde-Wright, R. Ransome and F. Sabatie, spokespersons JLab experiment E00-110.
46. P.-Y. Bertin, C. E. Hyde-Wright, F. Sabatie and E. Voutier, spokesperson JLab experiment E03-106.
47. V. Burkert, L. Elhouadrhiri, M. Garcon, S. Stepanyan, spokespersons JLab experiment E01-113.
48. R. Kaiser et al., “A large acceptance recoil detector for HERMES”, Addendum to the Proposal DESY PRC 97-07, HERMES 97-032.
49. N. D’Hose, Letter of intent for COMPASS, private communication.
50. “White Book”, *The Science driving the 12 GeV upgrade of CEBAF*, [http://www.jlab.org/div\\_dept/physics\\_division/GeV.html](http://www.jlab.org/div_dept/physics_division/GeV.html)